BMC Cardiovascular Disorders

RESEARCH

Open Access

Effects of low-dose radiation produced during radiofrequency ablation guided by 3D mapping on mitochondrial apoptosis in diabetic cardiomyocytes

Jia Gao[1†], Zhijun Meng[2†], Binghang Zhang[3], Nan Zhang[1], Min Guo[1], Meng Sun[1] and Rui Wang[1*]

Abstract

Background Three-dimensional (3D) mapping has been widely used in the clinical radiofrequency ablation of arrhythmia; however, the dose of intraoperative radiation exposure has not been determined. Moreover, whether a single instance of intraoperative radiation exposure has an effect on myocardial tissue or exacerbates diabetic heart injury remains uncertain.

Methods and results In this study, we evaluated the dose of intraoperative radiation generated during radiofrequency ablation via 3D mapping. ELISA, Western blot, flow cytometry, and oxygen consumption rate detection were used to identify the effects of the intraoperative radiation dose on cardiomyocyte apoptosis via the mitochondrial pathway and its specific mechanism. These results indicated that the exposure radiation used in radiofrequency ablation guided by 3D mapping for all types of arrhythmia was low-dose radiation (LDR; the doses were all less than 200 mGy). Although LDR (50, 100 and 200 mGy) had no significant effect on the mitochondrial apoptosis of normal cardiomyocytes, the 200 mGy radiation dose reduced the mitochondrial apoptosis of cardiomyocytes subjected to high glucose and high lipid (HG/HL) treatment. Mechanistically, an LDR of 200 mGy improved the expression of IL-10, reversed the accumulation of IL-6, ROS, disruption of $\Delta\psi m$, and the impairment of mitochondrial function caused by HG/HL. Additionally, 200 mGy radiation promoted the expression of Bcl-xl while reducing the expression of Bax in cardiomyocytes treated with HG/HL.

Conclusion In summary, this study demonstrated that the exposure radiation dose used in radiofrequency ablation guided by 3D mapping was low-dose radiation (LDR), which had no effect on the mitochondrial apoptosis pathway in normal cardiomyocytes and even had a protective effect on cardiomyocytes treated with HG/HL via increased IL-10 levels and the suppression of IL-6, ROS, and mitochondrial damage induced by HG/HL.

Highlights

- The exposure radiation dose of radiofrequency ablation guided by 3D mapping for all kinds of arrhythmia was low-dose radiation (less than 200 mGy).

†Jia Gao and Zhijun Meng contributed equally to this work.

*Correspondence:
Rui Wang
w4639551@126.com
Full list of author information is available at the end of the article

• LDR (50, 100 and 200 mGy) had no significant effect on the mitochondrial pathway in normal cardiomyocytes.

• Radiation (200 mGy) reduced mitochondrial apoptosis in myocardial cells after treatment with HG/HL by increasing IL-10 and suppressing the ROS, IL-6 and mitochondrial damage induced by HG/HL.

Keywords 3D mapping, Radiofrequency ablation, Low-dose radiation, Mitochondria apoptosis pathway, Mitochondrial damage

Introduction

During the initial period, accurate target localization in radiofrequency ablation was feasible for all types of arrhythmias by means of electrophysiological signals and fluoroscopy [1]. The adoption of 3D mapping systems, which are supposed to appropriately combine both anatomical and electrophysiological characteristics in recent years, has provided new therapeutic options for radiofrequency ablation of arrhythmias. It has great value for the diagnosis and ablation of cardiac arrhythmias and facilitates the diagnosis and treatment of complex arrhythmias [2]. These improvements can reduce procedural and fluoroscopic times, which leads to a decrease in radiation exposure in radiofrequency ablation [3, 4]. However, the radiation dose for radiofrequency ablation under the 3D mapping system has not been determined.

Like all ionizing radiation (IR), fluoroscopy is a major hurdle in operation [5]. Exposure to IR during cardiac catheterization may have harmful consequences for patients and the medical staff involved in the procedures [6]. Clinical and experimental results consistently demonstrate that the risk of heart disease is distinctly increased in people exposed to IR [7]. The myocardial tissue of patients who undergo radiofrequency ablation is closest to the radiation source used during the operation [8]. Whether the radiation generated during radiofrequency ablation guided by 3D mapping has a negative effect on the patient's heart is unknown. In addition, diabetes has become a public health issue and increases the risk of cardiac arrhythmias. Approximately 20% of patients with atrial fibrillation also have diabetes mellitus [9]. Some studies have shown that the heart tissue of diabetic patients is more vulnerable to IR [10–12]. While, studies indicate that low dose radiation (LDR) prevents diabetic cardiomyopathy and in normal cardiomyocytes, LDR induces slight changes in oxidative responses [13, 14]. Therefore, the effect of the intraoperative radiation dose on normal or diabetic cardiomyocytes is still unknown and the molecular mechanisms responsible for radiation in diabetes is still not fully understood.

Apoptosis plays an important role in maintaining many cellular functions, such as cell fragmentation and heterophagy [15]. Mitochondria play a crucial role in regulating cell death and appear to be the central executioners of apoptosis [16, 17]. The mitochondrial pathways of apoptosis are essential during the development of multitudinous cardiovascular diseases, such as coronary heart disease, radiotherapy-induced cardiomyopathy, and heart failure [18]. Radiation increases the release of inflammatory mediators, which leads to oxidative stress and mitochondrial apoptosis and is reduced by the interleukin-1β-blocking agent canakinumab [19]. Therefore, determining the mechanism underlying the effect of the dose of radiation produced during 3D-guided radiofrequency ablation and exploring the effects of radiation on myocardial cells may be promising therapeutic tools for treating cardiovascular disease.

We hypothesized that the intraoperative radiation generated during radiofrequency ablation via 3D mapping affects the mitochondrial apoptosis of cardiomyocytes and can also affect the diabetic myocardium. Therefore, the purposes of this study were 1) to identify the dose of intraoperative radiation generated during radiofrequency ablation under 3D mapping, 2) to detect the effect of the intraoperative radiation dose on normal or diabetic cardiomyocytes, and 3) to clarify its specific molecular mechanism.

Materials and methods

Radiation dose measurements in patients

A total of 280 patients (182 men and 98 women) were enrolled in this study. These patients first underwent radiofrequency ablation due to a variety of arrhythmias, including frequent ventricular premature beat (FVPB) (43), paroxysmal supraventricular tachycardia (PSVT) (128), atrial fibrillation (AF) (57), atrial flutter (AFL) (27) and other types of arrhythmias (25). Radiofrequency ablation was guided by 3D mapping (CARTO®, Biosense Webster Inc., Diamond Bar, CA, USA), and fluoroscopic guidance was provided with a Philips C biplane image intensifier system (Philips, Cleveland, USA). We collected data regarding the release of kinetic energy from air in matter (Kerma), which was measured in milligrays (mGy) [3]. Blood samples were randomly collected preoperatively and immediately postoperative for the detection of related inflammatory factors, including IL-2, IL-4, IL-6, IL-10, TNF-α and IFN-γ. The dose of radiation was obtained from the C biplane workstation. All study protocols were approved by the Ethics Committee of the First Hospital of Shanxi Medical University in accordance

with the Declaration of Helsinki (K-SK033). Written informed consent was obtained from all the subjects prior to study inclusion.

Cell culture and treatments

Human cardiomyocyte-like AC16 cells were purchased from American Type Culture Collection (ATCC; Rockville, MD, U.S.A.). All the cell lines were authenticated by short tandem repeat (STR) profiling and were routinely tested for Mycoplasma contamination. Foetal bovine serum was obtained from CellMax (Beijing, China, #SA211.02). All other cell culture-related reagents were purchased from Boster Biological Technology (Wuhan, China). AC16 cells were cultured in cardiocellular growth medium containing 10% foetal bovine serum, 2 mM glutamine, 100 U/ml penicillin and 100 μg/ml streptomycin in a humidified atmosphere of 5% CO_2 at 37 °C. Foetal bovine serum was obtained from CellMax (Beijing, China; #SA211.02). All other cell culture-related reagents were purchased from Boster Biological Technology (Wuhan, China). The AC16 cells were randomized to receive the following treatments after reaching 80% confluence: the control group (normal glucose/normal lipid, control, normal glucose containing 5.5 mM D-glucose + 19.5 mM L-glucose) and the high glucose/high lipid group (HG/HL, 25 mM D-glucose/250 μM palmitate, 24 h incubation) [20]. The cells were then directly irradiated under the X-ray emitter after HG/HL intervention for 24 h. The dose of the radiation (50, 100 or 200 mGy) was checked according to the metre on the X-ray emitter [21, 22].

Enzyme-linked immunosorbent assay

The level of IL-6 in the cell culture supernatant was determined via human IL-6 ELISA kits (Abcam, ab178013; Shanghai, China). The level of IL-10 in the cell culture supernatant was determined via human IL-10 ELISA kits (Abcam, ab185986; Shanghai, China) following the manufacturer's instructions.

Western blotting

A total of 50 μg of total protein per sample was separated via gel electrophoresis and transferred to polyvinylidene fluoride (PVDF) membranes followed by blocking with 5% skim milk at room temperature for 1 h. Then, the membranes were incubated with the appropriate primary antibodies against cleaved caspase-3/caspase-3 (dilution, 1:1000; Cell Signaling Technology, #9661/9662; Danvers, MA, U.S.A.), cleaved caspase-9/caspase-9 (dilution, 1:1000; Cell Signaling Technology, #9509/9504; Danvers, MA, U.S.A.), Bcl-xl (dilution, 1:1000; Abcam, ab32124; Cambridge, MA, U.S.A.), Bax (dilution, 1:1000; Abcam, ab182733, Cambridge, MA, U.S.A.), and β-Actin (dilution, 1:1000; BA2913, Boster, Shanghai, China) at 4 °C overnight. After washing with Tris-buffered saline with Tween (TBST) three times, the membranes were incubated with the secondary HRP-conjugated antibody (anti-mouse or anti-rabbit antibody, 1:10,000 dilution; Boster, Shanghai, China) for 1 h. Images were captured on a ChemiDoc MP Imaging System (Bio-Rad, CA, USA), and the density was quantified with ImageJ (NIH).

Flow cytometry

The intracellular reactive oxygen species (ROS) level was measured via a ROS assay kit (Jiancheng Bioengineering Institute, Nanjing, China) based on 2′,7′-dichlorodihydrofluorescein diacetate (DCFH-DA) staining following the manufacturer's instructions. Cell apoptosis was determined with an Annexin V-FITC Apoptosis Detection Kit (KeyGEN BioTECH, KGA105, Nanjing, China). After treatment, the cells were collected via trypsin digestion without ethylene diamine tetraacetic acid (EDTA), washed in phosphate-buffered saline (PBS) and resuspended in 200 μl of binding buffer. Then, the cells were stained with 5 μl of Annexin V-FITC, 5 μl of propidium iodide or 5 μl of DCFH-DA. Following incubation for 30 min at 37 °C in the dark, the cells were subjected to a FACS cell flow cytometer (BD Biosciences) equipped with CellQuest software.

The measurement of JC-1 or 5,5′,6,6′-tetrachloro-1,1′,3,3′-tetraethyl-imidacarbocyanine in cells was performed with a JC-1 Mitochondrial Membrane Potential Fluorescent Probe (YEASEN Biotech, 40705ES03, Shanghai, China). A decrease in the mitochondrial membrane potential indicates the early stage of apoptosis. At high mitochondrial membrane potentials, JC-1 aggregates in the mitochondrial matrix and forms J-aggregates, which can produce red fluorescence. At a low mitochondrial membrane potential, JC-1 cannot accumulate in the matrix of mitochondria, and JC-1 is a monomer that can produce green fluorescence. After treatment, the cells were collected via trypsin digestion without EDTA, washed in PBS and resuspended in 500 μl of JC-1 working medium in the dark. After incubation for 15–30 min in the dark, the cells were centrifuged and resuspended in 0.5 ml of PBS. The following flow analysis was performed via a FACS cell flow cytometer (BD Biosciences) equipped with CellQuest software.

Oxygen consumption rate detection

Oxygen consumption rate (OCR) measurements were performed via Seahorse XF96 Extracellular Flux and software (Seahorse Biosciences, North Billerica, MA). The mitochondrial respiration was monitored in real time according to a previous report [23]. Approximately 6×10^3 cells in 80 μL of cell culture growth medium

were seeded per well in a Seahorse XFp Cell Culture Miniplate and allowed to adhere overnight in a 37 °C humidified incubator with 5% CO_2. The cells were randomized to receive the treatments for 24 h after adherence. In addition, the sensor cartridge was hydrated in an Agilent Seahorse extracellular flux (XF) calibrant at 37 °C in a non-CO_2 incubator overnight. On the day of analysis, the assay medium was prepared with XF base medium (102353–100), 1 mM pyruvate, 2 mM glutamine, and 10 mM glucose (adjusted to pH 7.4 at 37 °C). The cells were washed three times with the assay medium described above, and the cell culture miniplates were placed in a 37 °C incubator without CO2 for 1 h prior to the assay. Simultaneously, 1.5 μM oligomycin, 1.0 μM trifluoromethoxy carbonylcyanide phenylhydrazone, carbonyl cyanide 4-(trifluoromethoxy) phenylhydrazone (FCCP), and 0.5 μM rotenone/antimycin A were prepared with the assay medium and loaded into the ports on the sensor cartridge. The loaded XF sensor cartridge with the XF utility plate was subsequently placed into the analyser and calibrated. After calibration, the utility plate was removed, and the Seahorse XFp Cell Culture Miniplate was placed on the tray. The basal OCR, ATP production-linked, maximal, proton leak-linked OCR, spare respiratory capacity and nonmitochondrial respiration were subsequently detected.

Statistical analysis

Statistical analyses were conducted using GraphPad Prism 10. Data normality was assessed via the Shapiro–Wilk test. For normally distributed data with three or more groups, one-way analysis of variance (ANOVA) followed by post-hoc multiple comparisons tests was employed. In cases involving two categorical independent variables affecting a continuous dependent variable or multiple groups over time, two-way ANOVA was utilized, complemented by Tukey's post-hoc multiple comparison test. Post-hoc comparisons were annotated with adjusted *P*-values to indicate statistical significance in the graphical representations. Normally distributed data are presented as mean ± standard error of the mean (SEM). Non-normally distributed data or those with sample sizes less than six were analyzed using non-parametric methods, specifically the Kruskal–Wallis test and Dunn's multiple post-hoc comparison test. These data are reported as median values with 95% confidence intervals. Survival analysis was performed using Kaplan–Meier curves and log-rank tests. This study did not employ full or cross-test multiple testing corrections; instead, local corrections were applied when necessary.

The sample size for each group represents the number of independent experimental units, determined based on prior experience and power analysis using a two-tailed Student's t-test to ensure detection of at least a 20% difference, assuming a statistical power of 80% ($\beta = 0.80$) and an alpha level of 0.05. All samples were included in the analysis without exclusions. Statistical significance was defined as a two-tailed *P* value less than 0.05.

Results

Low-dose radiation of radiofrequency ablation was established via 3D mapping

Arrhythmia patients (FVPB, supraventricular tachycardia, atrial fibrillation, ventricular tachycardia, etc.) were recruited for this study from January 2019 to June 2021 at the First Hospital of Shanxi Medical University. The exposure radiation dose of radiofrequency ablation guided by 3D mapping was analysed. The results shown in Table 1 indicate that the exposure radiation dose for atrioventricular nodal reentrant tachycardia (AVNRT) was 77.58 mGy, that for atrioventricular reentrant tachycardia (AVRT) originating from the left accessory pathway was 145.10 mGy, and that for the right accessory pathway was 85.66 mGy. The FVPB stemming from the left ventricle was 190 mGy, and that from the right ventricle was 60.42 mGy. The incidence of paroxysmal atrial fibrillation (PAF) was 146.20 mGy, persistent atrial fibrillation (PeAF) was 198.00 mGy, typical atrial flutter (AFL) was 179.2 mGy, atypical AFL was 188.26 mGy, and other types of arrhythmia (including atrial tachycardia and ventricular tachycardia) were 78.91 mGy (Table 1).

According to the results above, we found that the radiation dose of radiofrequency ablation with 3D mapping applied in various arrhythmia patients was lower than 200 mGy. The definition of LDR has been proposed to be below 200 mGy depending on the effects on the cardiovascular system [7]. In view of this, LDR was employed in the following experiments. High-dose radiation is detrimental to cardiovascular disease [24]; however, the effect of low-dose radiation on cardiovascular disease has not been investigated intensively. Recently, accumulating evidence has demonstrated that LDR has potential as a protective effect on myocardial tissue under certain circumstances [14]. Therefore, we focused on the effect of LDR on myocardial tissue in subsequent experiments.

LDR (200 mGy) decreased IL-6 and increased IL-10 in diabetic patients with hyperlipidaemia

Radiation leads to the release of inflammatory mediators, but whether LDR leads to the release of inflammatory mediators is unknown. The above arrhythmia patients were divided into a normal group and a diabetic with hyperlipidaemia (DH) group according to blood glucose/lipid and were roughly divided into 50 mGy, 100 mGy and 200 mGy according to the dose of intraoperative radiation. We retained the

Table 1 The radiation dose and DAP of radiofrequency ablation guided by 3D mapping for all kinds of arrhythmia

Variables	PVST			FVPB		AF		AFL		Other types (*n* = 25)
	AVNRT (*n* = 63)	AVRT		Left (*n* = 23)	Right (*n* = 20)	Paroxysmal (*n* = 42)	Persistent (*n* = 15)	Typical (*n* = 21)	Atypical (*n* = 6)	
		Left (*n* = 42)	Right (*n* = 23)							
Radiation dose(mGy)	77.58 ± 11.19	145.1 ± 19.26	85.66 ± 26.94	190 ± 36.00	60.42 ± 15.87	146.2 ± 15.57	198 ± 31.37	179.2 ± 11.69	188.26 ± 12.65	78.91 ± 24.27

PSVT Paroxysmal supraventricular tachycardia, *AVNRT* Atrioventricular nodal reentrant tachycardia, *AVRT* Atrioventricular reciprocating tachycardia, *FVPB* Frequent ventricular premature beat, *AF* Atrial fibrillation, *AFL* Atrial flutter

preoperative and immediate postoperative serum of the patients for the detection of related inflammatory mediators, including IL-2, IL-4, IL-6, IL-10, TNF-α and IFN-γ. The characteristics of the patient population are shown in Table 2. After analysing the results, we found that patients with DH presented an increase in IL-6 and a decrease in IL-10, while LDR decreased IL-6 and increased the expression of IL-10, and 200 mGy reversed the increase in IL-6 ($P=0.0058$) and decrease in IL-10 induced by DH ($P=0.002$) (Fig. 1A-B). However, no significant differences in the levels of IL-2, IL-4, TNF-α or IFN-γ were detected. To further verify the above experimental results, we used control and HG/HL-treated cardiomyocytes, irradiated them with different doses of radiation (50, 100 and 200 mGy), collected the supernatants of the cells for IL-6 and IL-10 ELISA detection, and obtained the same results ($P=0.0112$ and $P=0.0045$) (Fig. 1C-D).

Table 2 The characteristics of Patient population

	Normal				Diabetic with hyperlipidaemia				*P* value
	0 mGy	50 mGy	100 mGy	200 mGy	0 mGy	50 mGy	100 mGy	200 mGy	
Gender	14/13	8/5	6/8	8/6	7/7	4/9	7/6	7/6	
Age(year)	63.19 ± 2.084	57.08 ± 3.668	67.36 ± 2.475	64.29 ± 2.673	63.21 ± 2.518	63.38 ± 3.419	67.54 ± 2.330	61.38 ± 2.360	0.2324
BMI	25.35 ± 0.7317	25.38 ± 0.5129	24.65 ± 1.119	23.14 ± 1.095	26.72 ± 0.9481	24.56 ± 0.8715	23.45 ± 0.9240	26.10 ± 0.8563	0.1110
FBG	4.776 ± 0.1184	4.658 ± 0.1951	4.436 ± 0.1790	4.935 ± 0.1769	8.948 ± 0.6923	9.763 ± 0.7604	8.719 ± 0.6481	8.964 ± 0.7391	< 0.0001
TC	3.572 ± 0.1368	3.746 ± 0.2295	3.149 ± 0.3714	3.504 ± 0.1672	6.294 ± 0.3559	6.848 ± 0.3819	6.036 ± 0.3857	6.204 ± 0.3338	< 0.0001
TG	1.064 ± 0.08904	0.9900 ± 0.1134	1.157 ± 0.3026	1.076 ± 0.0830	2.657 ± 0.3378	3.778 ± 0.6224	2.817 ± 0.3190	2.948 ± 0.5651	< 0.0001
LDL	2.109 ± 0.0956	2.344 ± 0.1357	1.856 ± 0.3069	2.027 ± 0.1311	3.800 ± 0.1915	3.823 ± 0.2564	3.600 ± 0.1697	3.893 ± 0.1525	< 0.0001

BMI Body mass index, *FBG* Fasting blood-glucose, *TC* Cholesterol, *TG* Triglyceride, *LDL* Low density lipoprotein

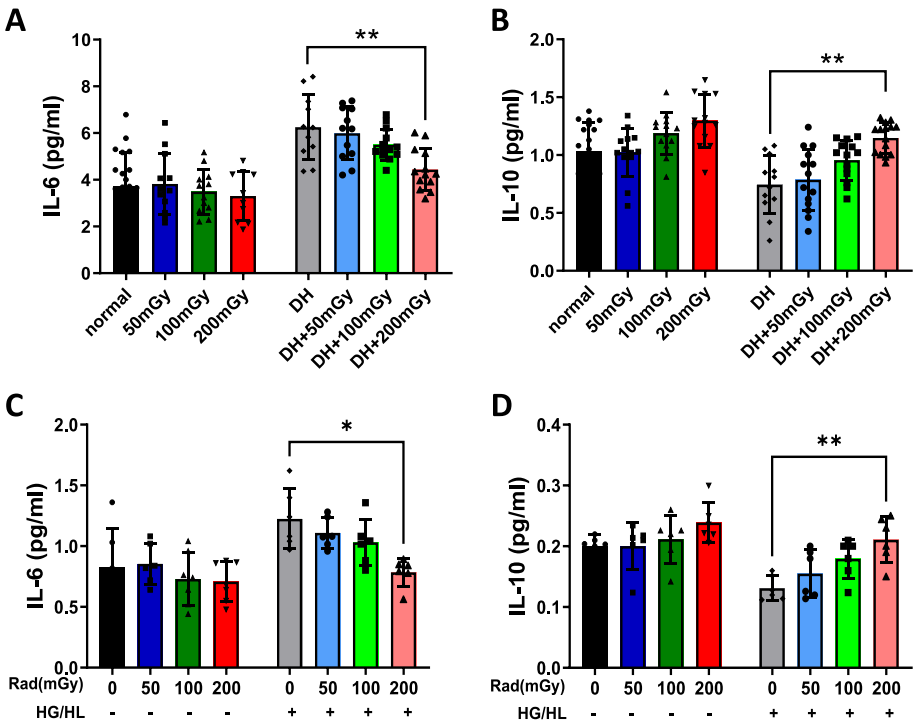

Fig. 1 Detection of IL-6 and IL-10. **A** IL-6 levels in patients were determined by ELISA. $n=13$–21/group. **B** IL-10 levels in patients were determined by ELISA. $n=13$–20/group. **C** IL-6 levels were determined by ELISA in cardiomyocytes subjected to control or HG/HL conditions with or without LDR. $n=6$/group. **D** IL-10 was determined by ELISA in cardiomyocytes subjected to control conditions or HG/HL conditions with or without LDR. $n=6$/group. ** $P<0.01$ vs. the DH group, **$P<0.01$ vs. the HG/HL group. Statistical significance was evaluated by one-way ANOVA. Tukey tests were used to correct for multiple comparisons. LDR, low-dose radiation; DH, diabetic with hyperlipidaemia; HG/HL, high glucose/high lipid

LDR (200 mGy) reduced the degree of apoptosis induced by HG/HL

Since cell apoptosis plays a considerable role in the occurrence and development of cardiovascular diseases, we sought to investigate whether the LDR generated during radiofrequency ablation guided by 3D mapping was involved in myocardial apoptosis. The following experiments were conducted. First, the effect of LDR on myocardial apoptosis was analysed via flow cytometry (FCM). 24 h after treatment, apoptosis was determined. In normal cardiomyocytes, LDR appeared to promote cardiomyocyte apoptosis, however, no difference in apoptosis was detected between the control group with or without LDR, statistical analysis did not reveal significant differences. In contrast, the rate of cardiomyocyte apoptosis was significantly elevated following HG/HL intervention. Whereas, the administration of LDR tended to reduce cardiac apoptosis in the HG/HL group. Most importantly, the radiation dose of 200 mGy significantly attenuated cardiac apoptosis compared with that in the HG/HL group ($P=0.0322$) (Fig. 2A-B). These results indicated that the administration of LDR reduced apoptosis in the HG/HL group but did not affect the occurrence of apoptosis in normal cardiomyocytes which suggest that LDR

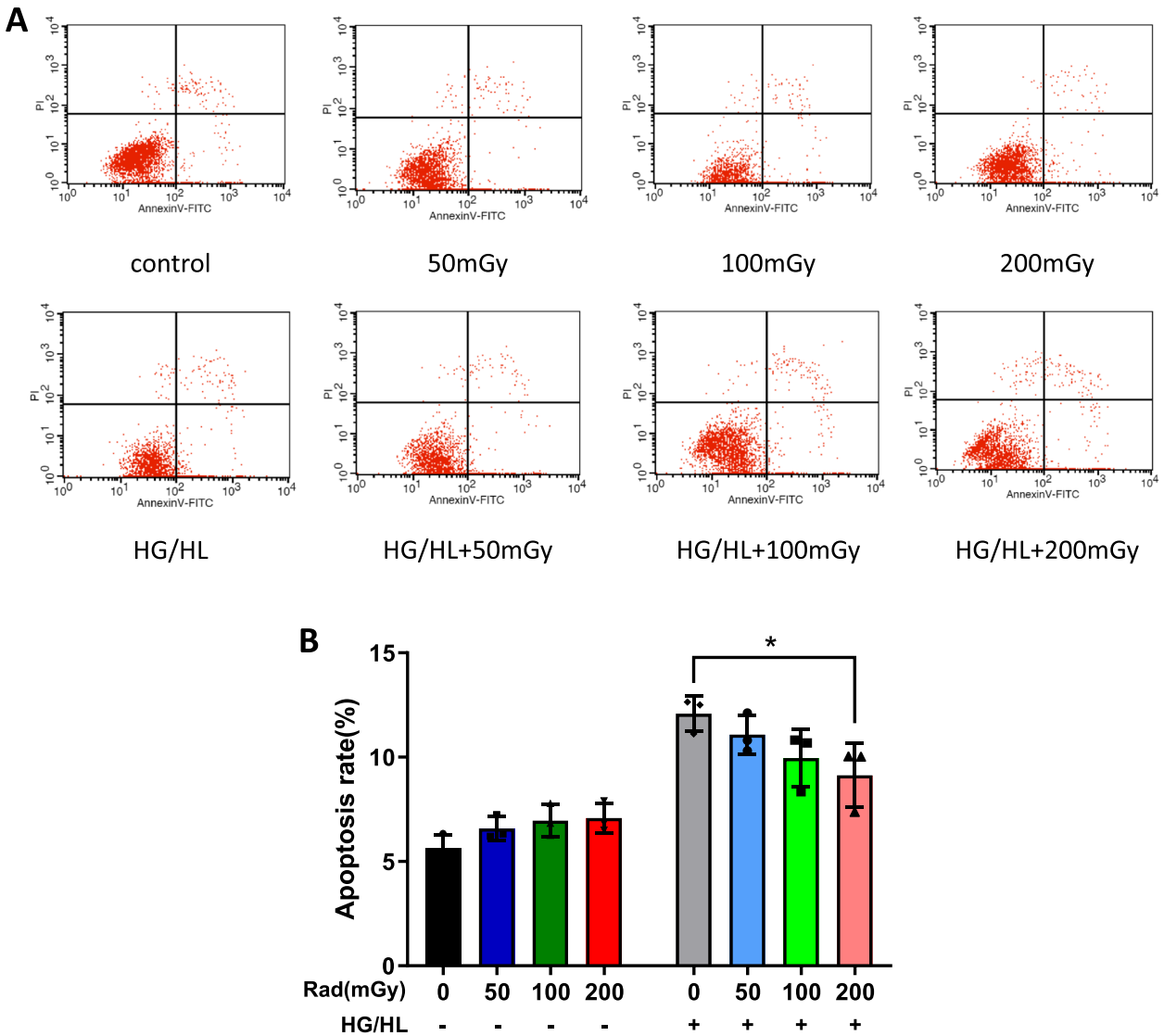

Fig. 2 LDR regulates cardiomyocyte apoptosis in response to HG/HL treatment. **A** Apoptosis was determined by flow cytometry in cardiomyocytes subjected to control or HG/HL conditions with or without LDR. **B** Quantification of the rate of apoptosis. The data are representative of 3 biological replicates. $^{**}P<0.01$ vs. the HG/HL group. Statistical significance was evaluated via one-way ANOVA. Tukey tests were used to correct for multiple comparisons. LDR, low-dose radiation; HG/HL, high glucose/high lipid

may potentially inhibit the progression of clinical diabetic cardiomyopathy; however, the precise mechanism remains to be elucidated.

Therefore, we sought to investigate the downstream signalling pathways contributing to the LDR-induced antiapoptotic effect. Several mitochondrial apoptosis-related cytokines play important roles in myocardial cell apoptosis. The ratios of cleaved caspase-3/caspase-3 and cleaved caspase-9/caspase-9 were measured in myocardial cells after exposure to different doses of radiation. Similarly, 200 mGy reduced the ratio of cleaved caspase-3/caspase-3 ($P=0.0117$) and cleaved caspase-9/caspase-9 ($P=0.0089$) in cardiomyocytes subjected to HG/HL treatment. However, no significant differences in cleaved caspase-3/caspase-3 or cleaved caspase-9/caspase-9 were detected in the control groups (Fig. 3A-B, D-E). These results indicate that mitochondrial apoptosis is involved in the LDR-induced antiapoptotic effect.

Next, to obtain evidence that LDR regulates cardiomyocyte apoptosis, Bcl-xl and Bax were measured.

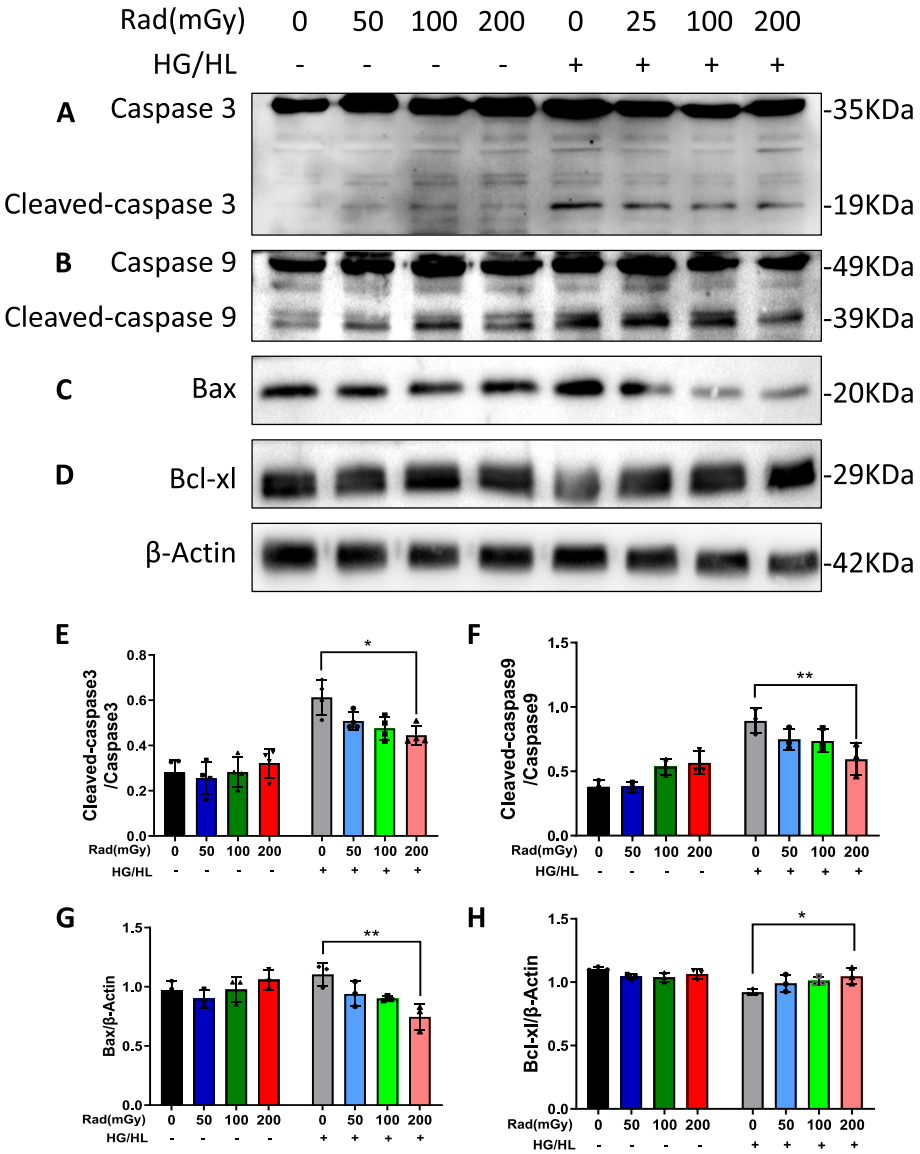

Fig. 3 Mitochondrial apoptosis protein detection in cardiomyocytes. Cleaved caspase 3 (**A**), cleaved caspase-9/caspase-9 (**B**), Bax (**C**), and Bcl-xl (**D**) were evaluated by Western blot in control or HG/HL-treated cardiomyocytes with or without LDR. **E-H** The densities of caspase-3/caspase-3, cleaved caspase-9/caspase-9, Bax and Bcl-xl were quantified. The data are representative of 3 biological replicates. *$P<0.05$, **$P<0.01$ vs. the HG/HL group. Statistical significance was evaluated by one-way ANOVA. Tukey tests were used to correct for multiple comparisons. LDR, low-dose radiation; HG/HL, high glucose/high lipid

Consistent with the results above, the expression of Bax was lower in the HG/HL group with the 200 mGy radiation dose ($P=0.0032$), whereas the expression of Bcl-xl was greater in the HG/HL group with the 200 mGy radiation dose than in the HG/HL group ($P=0.0310$). Similarly, the expression of Bax and Bcl-xl did not significantly change in the control groups regardless of exposure to radiation. These results demonstrate that 200 mGy radiation upregulates antiapoptotic proteins and downregulates proapoptotic proteins in diabetic myocardiocytes but not in normal myocardiocytes.

LDR at 200 mGy reversed the accumulation of ROS, disruption of Δψm, and the impairment of mitochondrial function caused by HG/HL

Mitochondrial damage plays a key role in cellular mitochondrial apoptosis largely through the production of reactive oxygen species (ROS). As our in vitro results indicate that an LDR of 200 mGy attenuated apoptosis, we next focused on the antioxidative properties of the LDR. Several experiments were executed as follows. First, FCM was performed to observe the effect of LDR on intracellular ROS accumulation. As shown in Fig. 4A-B, there was no significant effect on ROS accumulation in the control groups with or without radiation. Consistent with the results of apoptosis, the

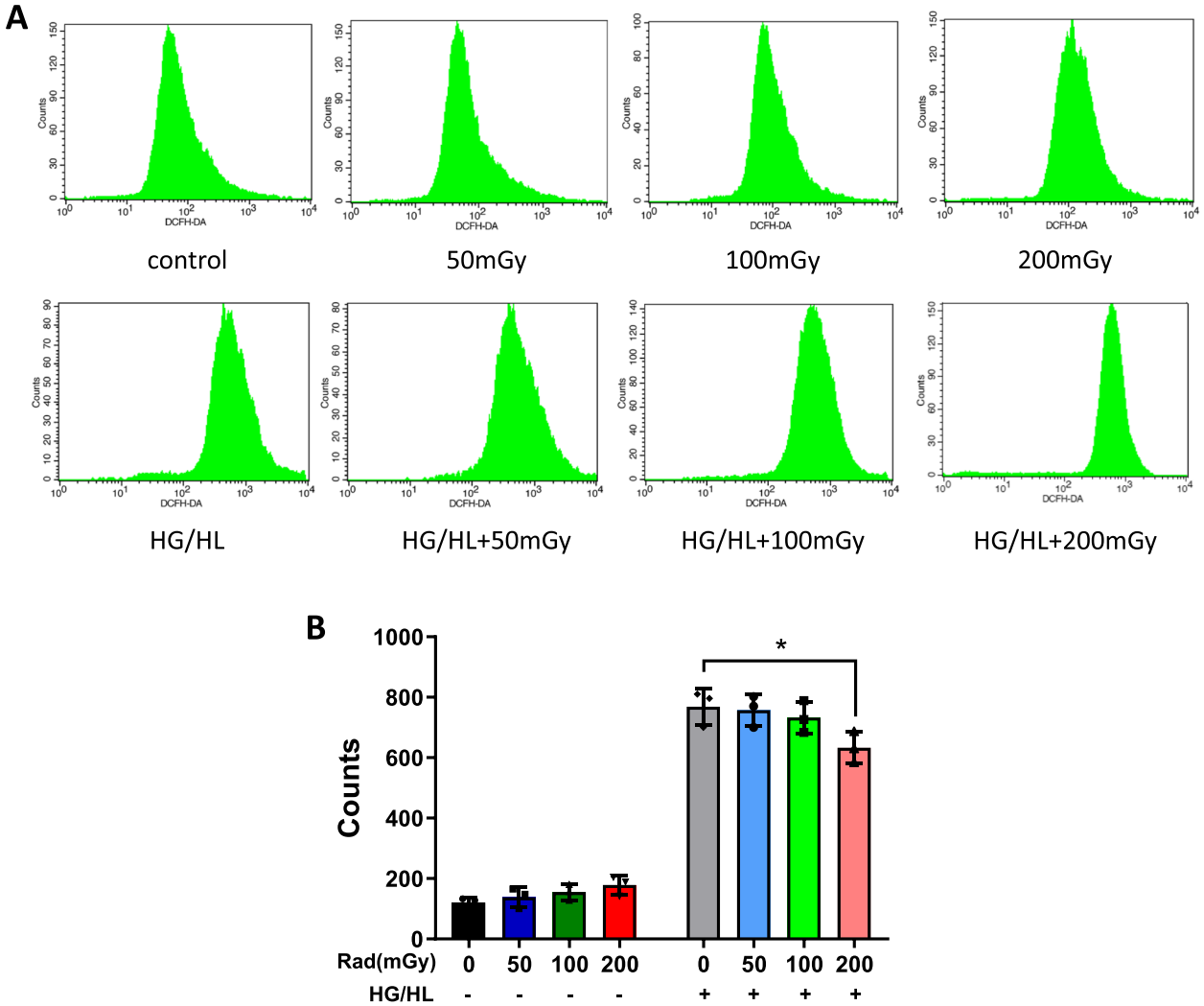

Fig. 4 ROS evaluated in cardiomyocytes. **A** DCFH-DA staining was determined by flow cytometry in control or HG/HL-treated cardiomyocytes with or without LDR. **B** Quantification of ROS production. The data are representative of 3 biological replicates. *$P<0.05$ vs. the HG/HL group. Statistical significance was evaluated by one-way ANOVA. Tukey tests were used to correct for multiple comparisons. ROS, reactive oxygen species; LDR, low-dose radiation; HG/HL, high glucose/high lipid

LDR of the 200 mGy radiation group slightly reversed the increase in ROS induced by HG/HL ($P=0.0239$). Second, to identify whether LDR causes mitochondrial dysfunction, we evaluated the effect of LDR on mitochondrial function in cardiomyocytes treated with control or HG/HL. Changes in mitochondrial membrane potential (Δψm) in cardiomyocytes treated with LDR or HG/HL were assessed with JC-1 via FCM. As shown in Fig. 5A-B, no significant effect on JC-1 was detected in control or HG/HL cardiomyocytes with 50 or 100 mGy radiation. However, 200 mGy radiation reversed the increase in JC-1 induced by HG/HL ($P=0.0152$), but not in control cardiomyocytes.

Third, in an attempt to prove the antioxidative effect of LDR under diabetic conditions, a Seahorse XF24 analyser was used to confirm the oxygen consumption rate (OCR) of cardiomyocytes in the LDR on mitochondrial aerobic metabolism. As shown in Fig. 6A-F, no statistically significant differences were detected in the mitochondrial respiration parameters (nonmitochondrial oxygen consumption, basal respiration, maximal respiration and ATP production) of the control groups with

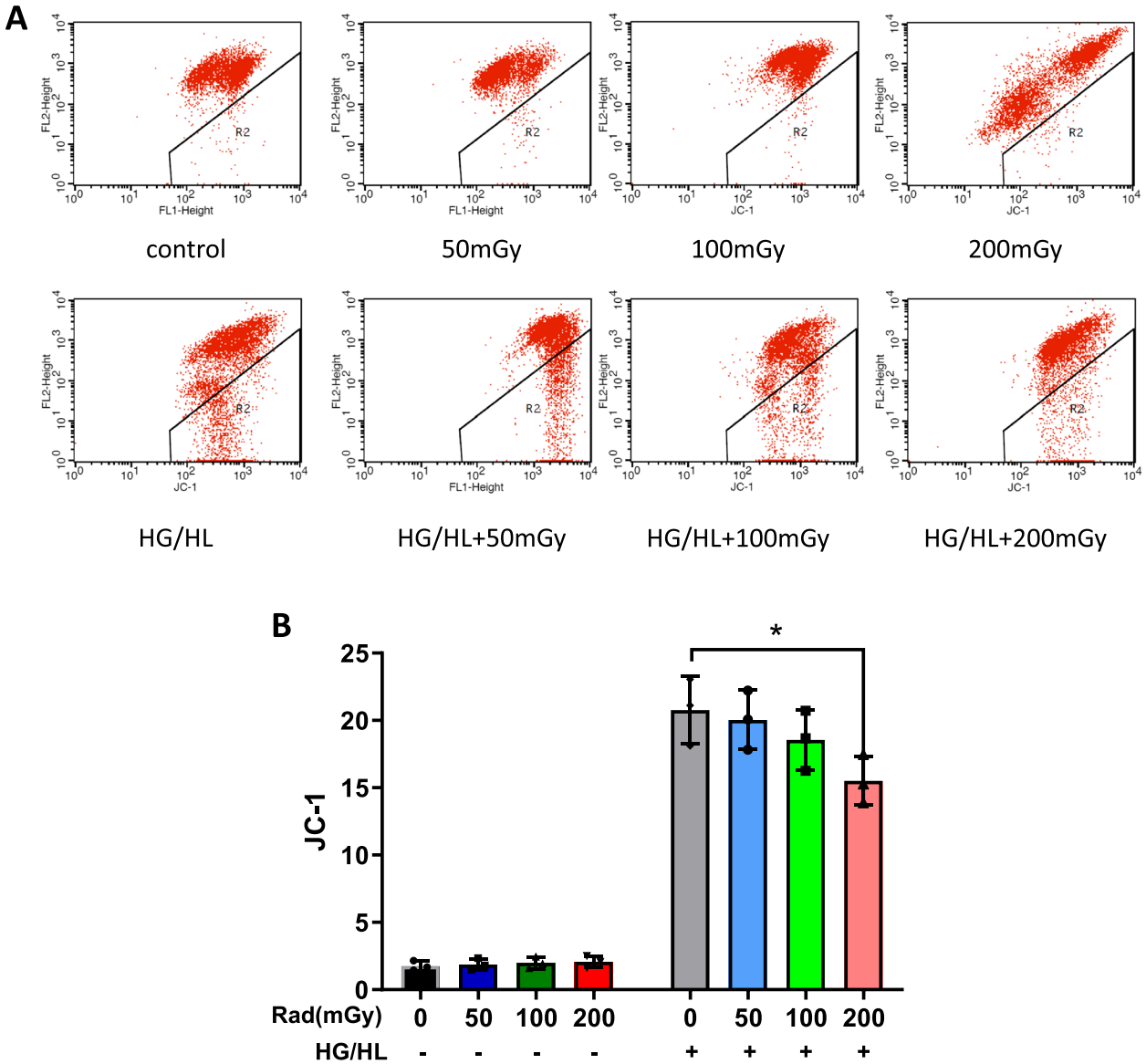

Fig. 5 LDR effects on mitochondrial function in cardiomyocytes treated with control or HG/HL. The mitochondrial membrane potential (Δψm) was assessed by JC-1 using flow cytometry in control or HG/HL-treated cardiomyocytes with or without LDR. **B** Quantification of JC-1. The data are representative of 3 biological replicates. $^{**}P<0.01$ vs. the HG/HL group. Statistical significance was evaluated by one-way ANOVA. Tukey tests were used to correct for multiple comparisons. Δψm, mitochondrial membrane potential; LDR, low-dose radiation; HG/HL, high glucose/high lipid

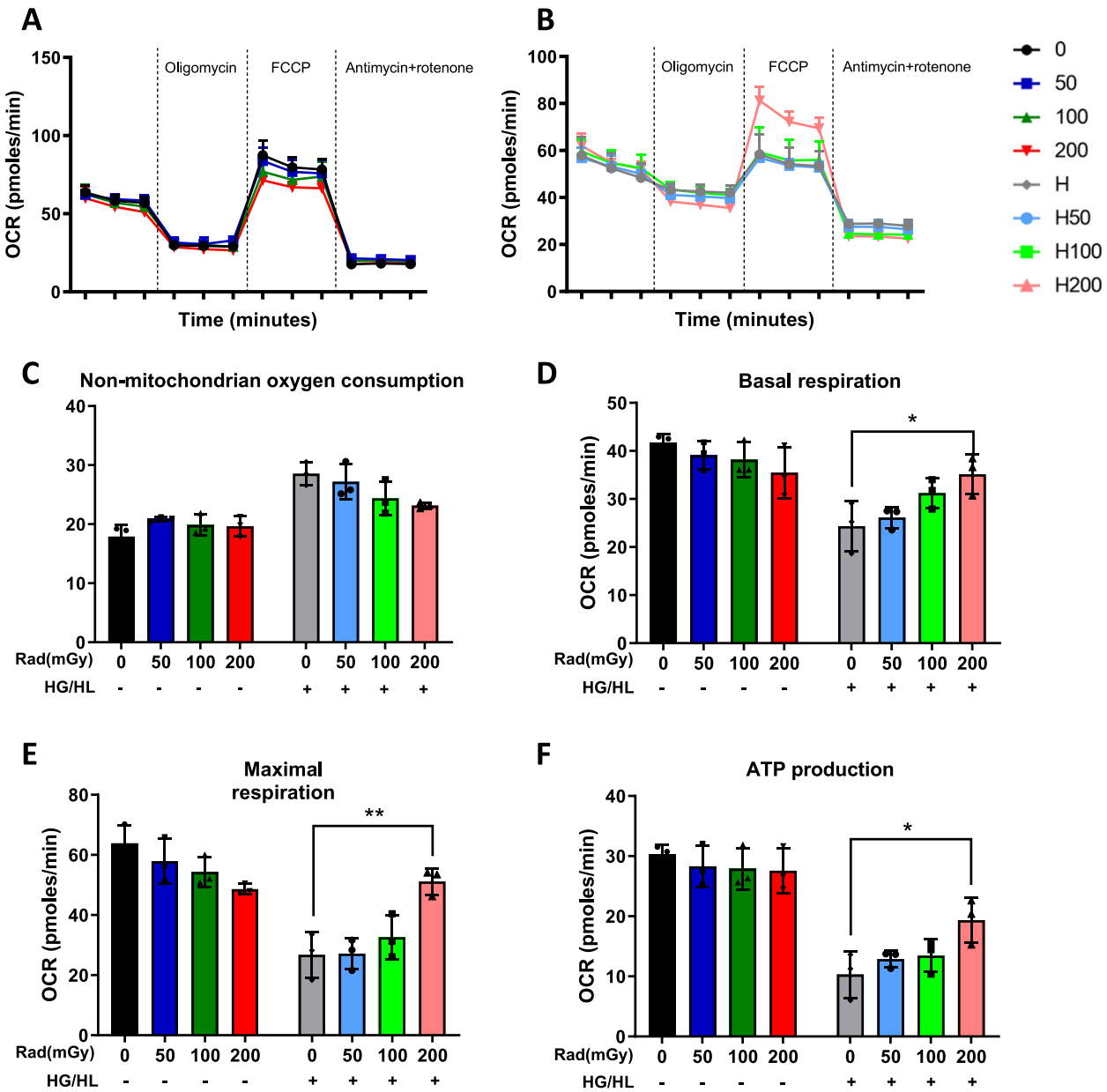

Fig. 6 Evaluation of LDR on cardiomyocyte mitochondrial aerobic metabolism. **A-B** Mitochondrial respiration, indicated as the oxygen consumption rate (OCR), was measured by a Seahorse XF96 Analyser in control or HG/HL-treated cardiomyocytes with or without LDR. Maximal respirations were determined by the sequential addition of oligomycin, FCCP, rotenone or antimycin A. The data are representative of 3 biological replicates. **C-F** Quantification of the capacity for nonmitochondrial oxygen consumption (**C**), basal respiration (**D**), maximal respiration (**E**) and ATP production (**F**). *$P < 0.05$ 200 mGy + HG/HL vs. HG/HL group. Statistical significance was evaluated by one-way ANOVA. Tukey tests were used to correct for multiple comparisons. LDR, low-dose radiation; HG/HL, high glucose/high lipid

or without LDR. Following HG/HL intervention, there was a significant reduction in mitochondrial respiration parameters of cardiomyocytes, including basal respiration, maximal respiration, and ATP production. Furthermore, an LDR of 200 mGy significantly reversed the reduction in the basal respiration ($P=0.0438$), maximal respiration ($P=0.0022$), and ATP production ($P=0.0433$) of HG/HL group, moreover, LDR had the most obvious effect on maximal respiration which was not detected in the 50 or 100 mGy groups. Taken together, these results demonstrated that an LDR of 200 mGy radiation, not 50 or 100 mGy, reduced ROS accumulation, mitochondrial membrane damage and respiratory function decline in cardiomyocytes in diabetic hearts which likely indicates

the clinical efficacy of LDR in inhibiting apoptosis in diabetic cardiomyopathy by safeguarding mitochondrial aerobic respiration through its anti-oxidative stress properties.

Discussion

Our research is the first to prove that the exposure radiation dose of radiofrequency ablation guided by 3D mapping for all kinds of arrhythmia is LDR (less than 200 mGy). Furthermore, this study demonstrated that LDR (50, 100 and 200 mGy) had no significant effect on the apoptosis of the mitochondrial pathway in normal cardiomyocytes; however, 200 mGy radiation reduced myocardial cell mitochondrial apoptosis after HG/HL treatment via the suppression of ROS and mitochondrial damage.

Nonetheless, we recognize that our study has several limitations. First, it is uncertain whether frequent exposure to LDR has any effect on the myocardial tissue of surgeons performing interventional surgery. Prolonged exposure to low-dose radiation, as experienced by medical personnel in radiology, has been demonstrated to influence thyroid function and elevate the risk of developing thyroid nodules [25]. Besides, in the context of the Fukushima nuclear accident, numerous studies have examined the effects of long-term LDR exposure on animals and ecosystems [26]. Although the primary focus has not been on cardiac muscle tissue, the research highlights that LDR can induce changes at the cellular and tissue levels, such as oxidative stress and DNA damage, which may potentially affect cardiac muscle tissue as well. Second, the health effects of radiation exposure include acute disorders and late onset disorders [37]. Our study revealed that LDR did not significantly affect the mitochondrial apoptosis of cardiomyocytes in the acute stage, but it is unknown whether there is a delayed effect on mitochondrial apoptosis. Finally, the antiapoptotic effect of LDR was not determined in diabetic animal models, and further research is needed in the future.

Before the use of 3D mapping, radiofrequency catheter ablation physicians experienced in performing the procedure required a significant amount of fluoroscopic imaging and resulted in a moderate amount of radiation exposure to both the patients undergoing the procedure and the physicians manipulating the electrode catheters [27]. Moreover, radiation exposure is responsible for increased sensitivity to injury in diabetic hearts [11]. Recently, radiofrequency ablation of various arrhythmias under 3D mapping has become increasingly prevalent in clinical radiofrequency ablation, including supracardial tachycardia, atrial arrhythmias, and complex ventricular arrhythmias, and has even achieved zero fluoroscopy (ZF) or near-ZF-guided catheter ablation for the treatment of arrhythmias in the paediatric or pregnant population [28–30]. The use of 3D mapping reduces the radio-exposure time and has no effect on the surgical success rate or complications of radiofrequency ablation in AVNRT patients [3]. However, few studies have concentrated on the statistical analysis of the radiation dose used during surgery and the effects of single radiation exposure on myocardial function in diabetic patients.

The negative effects of exposure to radiation on cardiovascular disease have been identified by long-term, large-scale epidemiological studies [7, 31]. A life expectancy study of Japanese atomic bomb survivors (LSSs) provided evidence that there is a certain relationship between the risk of circulatory disease and radiation dose; however, there is no definite linear relationship, especially at lower doses [32]. The impact of LDR remains a subject of considerable debate. While some studies have demonstrated beneficial effects [14, 33, 34], such as stimulatory responses, others have highlighted potential risks. The threshold for adverse effects and the influence of individual genetic variations on LDR responses remain areas of ongoing research and are not yet fully elucidated.

Multiple studies have highlighted the role of oxidative stress in radiation-induced cardiovascular damage, which is more severe in diabetic patients [11, 34, 35]. Mitochondria are target organelles of LDR and mitochondrial response influences radiation sensitivity in human cells [36]. LDR exert substantial effects on mitochondrial function, which subsequently influences cellular responses such as apoptosis, DNA repair, and the management of oxidative stress. While this radiation can potentially damage sensitive cells, it may also serve a protective role in certain contexts, including neurodegenerative diseases. Additional research is essential to comprehensively elucidate the mechanisms underlying the impact of LDR on mitochondrial biology and its potential therapeutic applications. Our findings provide new insights into cardiovascular risk estimation associated with LDR exposure. Accumulating studies support the concept that oxidative stress caused by elevated ROS, which may be improved by nanoencapsulation of Coenzyme Q10, is a potential mechanism governing the increased sensitivity of the diabetic heart [37, 38]. In addition, mitochondrial dysfunction contributes to oxidative stress, as it is both a target and a source of ROS [39].

In summary, our study revealed that the LDR generated during radiofrequency ablation under the guidance of 3D mapping does not alter the degree of apoptosis of the mitochondrial pathway in normal cardiomyocytes and can reverse HG/HL intervention in cardiomyocytes by reducing ROS and maintaining mitochondrial function. On the other hand, our study demonstrated that the protective effect of LDR on mitochondrial apoptosis induced

by HG/HL also prompt us that LDR may be a novel therapeutic target with potential for preventing diabetic cardiomyopathy. Nonetheless, several challenges and research gaps persist in the clinical application of LDR for diabetic cardiomyopathy. Notably, there is a lack of robust direct clinical evidence to substantiate its efficacy and safety. Furthermore, determining an optimal therapeutic dose remains critical, while long-term safety concerns, including potential risks such as carcinogenesis, must be rigorously assessed which is especially pertinent for diabetic patients who often have comorbid conditions.

Provide additional information

All study protocols were approved by the Ethics Committee of the First Hospital of Shanxi Medical University in accordance with the Declaration of Helsinki. Written informed consents were obtained from all subjects prior to study inclusion.

Authors' contributions

All authors contributed to the study conception and design. Material preparation, data collection and analysis were performed by Jia Gao. The first draft of the manuscript was written by Jia Gao, Zhijun Meng and Binghang Zhang, Nan Zhang, Min Guo, Meng Sun and Rui Wang revised it critically for important intellectual content. All authors read and approved the final manuscript.

Funding

This study was supported by The Cultivation Project of Young and Middle-aged Academic Leaders of the First Hospital of Shanxi Medical University (Grant/Award No. YD1609); The supporting funds for the "Introduction of Talents" doctoral program in the First Hospital of Shanxi Medical University from 2020–2021(Grant No. 09686#); Basic Research Program of Shanxi Province (Grant No. 202203021222378 and 202103021223418); National Natural Science Foundation of China for Young Scientists (Grant No. 82000426 and 82300492); Scientific Research Project of Health Commission in Shanxi Province (Grant No. 2023XG009 and 2023RC008); Project funded by China Postdoctoral Science Foundation (Grant No. 2023M732152 and 2023M732154); Research Project Supported by Shanxi Scholarship Council of China (Grant No. 2023–181) and Fund Program for the Scientific Activities of Selected Returned Overseas Professionals in Shanxi Province (Grant No. 20230054).

Data availability

The datasets used and/or analyzed during the current study are available from the corresponding author on reasonable request.

Declarations

Competing interests

The authors declare no competing interests.

Author details

[1]Department of Cardiology, First Hospital of Shanxi Medical University, Taiyuan, Shanxi 030001, China. [2]Department of Clinical Laboratory, Shanxi Provincial People's Hospital, Taiyuan, Shanxi, China. [3]The Second Clinical Medical College, Shanxi Medical University, Taiyuan, Shanxi, China.

Received: 20 August 2024 Accepted: 3 March 2025
Published online: 17 March 2025

References

1. Perisinakis K, et al. Accurate assessment of patient effective radiation dose and associated detriment risk from radiofrequency catheter ablation procedures. Circulation. 2001;104(1):58–62.
2. Yamamoto M, et al. Effectiveness of a 3D mapping benchmark for ablation in patients with atrioventricular nodal reentrant tachycardia. Pacing Clin Electrophysiol. 2020;43(12):1546–53.
3. Bagchi A, et al. How significant is the radiation exposure during electrophysiology study and ablation procedures for supraventricular tachycardia? Indian Heart J. 2021;73(2):221–2.
4. Christoph M, et al. Fluoroscopy integrated 3D mapping significantly reduces radiation exposure during ablation for a wide spectrum of cardiac arrhythmias. Europace. 2015;17(6):928–37.
5. Liu G, et al. Effect of low-level radiation on the death of male germ cells. Radiat Res. 2006;165(4):379–89.
6. Balter S, et al. Fluoroscopically guided interventional procedures: a review of radiation effects on patients' skin and hair. Radiology. 2010;254(2):326–41.
7. Puukila S, et al. Impact of Ionizing Radiation on the Cardiovascular System: A Review. Radiat Res. 2017;188(4.2):539–546.
8. Miłowska K, Grabowska K, Gabryelak T. Applications of electromagnetic radiation in medicine. Postepy Hig Med Dosw (Online). 2014;68:473–82.
9. Marx N, et al. 2023 ESC Guidelines for the management of cardiovascular disease in patients with diabetes. Eur Heart J. 2023;44(39):4043–140.
10. Nylander V, et al. Ionizing Radiation Potentiates High-Fat Diet-Induced Insulin Resistance and Reprograms Skeletal Muscle and Adipose Progenitor Cells. Diabetes. 2016;65(12):3573–84.
11. Dombrovska NS, et al. morphological and functional myocardial abnormalities in the chornobyl npp accident clean-up workers of «IODINE» period having got type 2 diabetes mellitus. Probl Radiac Med Radiobiol. 2018;23:302–30.
12. Bazyka OD, Bilyi DO. Diseases of circulatory system and comorbid type ii diabetes mellitus in the chornobyl accident consequences clean-up workers. Probl Radiac Med Radiobiol. 2018;23:246–53.
13. Yan X, et al. Cardiovascular risks associated with low dose ionizing particle radiation. PLoS ONE. 2014;9(10):e110269.
14. Zhang F, et al. Low-dose radiation prevents type 1 diabetes-induced cardiomyopathy via activation of AKT mediated anti-apoptotic and anti-oxidant effects. J Cell Mol Med. 2016;20(7):1352–66.
15. Xu X, Lai Y, Hua ZC. Apoptosis and apoptotic body: disease message and therapeutic target potentials. Biosci Rep. 2019;39(1):BSR20180992. https://doi.org/10.1042/BSR20180992 .
16. Annesley SJ, Fisher PR. Mitochondria in Health and Disease. Cells. 2019;8(7):680. https://doi.org/10.3390/cells8070680.
17. Chistiakov DA, et al. The role of mitochondrial dysfunction in cardiovascular disease: a brief review. Ann Med. 2018;50(2):121–7.
18. Davidson SM, et al. Mitochondrial and mitochondrial-independent pathways of myocardial cell death during ischaemia and reperfusion injury. J Cell Mol Med. 2020;24(7):3795–806.
19. Quagliariello V, et al. Interleukin-1 blocking agents as promising strategy for prevention of anticancer drug-induced cardiotoxicities: possible implications in cancer patients with COVID-19. Eur Rev Med Pharmacol Sci. 2021;25(21):6797–812.
20. Gan L, et al. Small Extracellular Microvesicles Mediated Pathological Communications Between Dysfunctional Adipocytes and Cardiomyocytes as a Novel Mechanism Exacerbating Ischemia/Reperfusion Injury in Diabetic Mice. Circulation. 2020;141(12):968–83.
21. Frieß JL, et al. Electrophysiologic and cellular characteristics of cardiomyocytes after X-ray irradiation. Mutat Res. 2015;777:1–10.
22. Gramatyka M, Skorupa A, Sokół M. Nuclear magnetic resonance spectroscopy reveals metabolic changes in living cardiomyocytes after low doses of ionizing radiation. Acta Biochim Pol. 2018;65(2):309–18.
23. Plitzko B, Loesgen S. Measurement of Oxygen Consumption Rate (OCR) and Extracellular Acidification Rate (ECAR) in Culture Cells for Assessment of the Energy Metabolism. Bio Protoc. 2018;8(10):e2850.
24. Kamiya K, et al. Long-term effects of radiation exposure on health. Lancet. 2015;386(9992):469–78.
25. FENG Chunyan WL. Adverse effects of long-term low-dose exposure to ionizing radiation on thyroid nodules of medical staff in radiology department. Occupational Health and Emergency Rescue. 2020;38(1):41–43.
26. Fukumoto M .Low-Dose Radiation Effects on Animals and Ecosystems: Long-Term Study on the Fukushima Nuclear Accident[J].Low-Dose Radiation Effects on Animals and Ecosystems, 2020. https://doi.org/10.1007/978-981-13-8218-5.

27. Calkins H, et al. Radiation exposure during radiofrequency catheter ablation of accessory atrioventricular connections. Circulation. 1991;84(6):2376–82.
28. Marazzato J, et al. Mapping and Ablation of Atypical Atrial Flutters. Card Electrophysiol Clin. 2022;14(3):471–81.
29. Watanabe N, Ashikaga K. Mitral regurgitation improvement after successful atrial fibrillation ablation by using a 3D mapping system. Ann Cardiothorac Surg. 2024;13(1):99–101.
30. Prana Jagannatha GN, et al. Safety and feasibility of 3D-electroanatomical mapping-guided zero or near-zero fluoroscopy catheter ablation for pediatric arrhythmias: Meta-analysis. J Arrhythm. 2024;40(4):913–34.
31. Lenneman CG, Sawyer DB. Cardio-Oncology: An Update on Cardiotoxicity of Cancer-Related Treatment. Circ Res. 2016;118(6):1008–20.
32. Shimizu Y, et al. Radiation exposure and circulatory disease risk: Hiroshima and Nagasaki atomic bomb survivor data, 1950–2003. BMJ. 2010;340:b5349.
33. Song KH, Jung SY, Park JI, Ahn J, Park JK, Hwang SG, Kim EH, Nam SY, Park S, Ha H, Song JY. Evaluation of Anti-Tumor Effects of Whole-Body Low-Dose Irradiation in Metastatic Mouse Models. Cancers (Basel). 2020;12(5):1126. https://doi.org/10.3390/cancers12051126.
34. Jiang X, et al. Low dose radiation prevents doxorubicin-induced cardiotoxicity. Oncotarget. 2018;9(1):332–45.
35. Azzam EI, Jay-Gerin JP, Pain D. Ionizing radiation-induced metabolic oxidative stress and prolonged cell injury. Cancer Lett. 2012;327(1–2):48–60.
36. Shimura T, et al. Severe mitochondrial damage associated with low-dose radiation sensitivity in ATM- and NBS1-deficient cells. Cell Cycle. 2016;15(8):1099–107.
37. Senoner T, Dichtl W. Oxidative Stress in Cardiovascular Diseases: Still a Therapeutic Target? Nutrients. 2019;11(9):2090. https://doi.org/10.3390/nu11092090.
38. Quagliariello V, et al. Nano-Encapsulation of Coenzyme Q10 in Secondary and Tertiary Nano-Emulsions for Enhanced Cardioprotection and Hepatoprotection in Human Cardiomyocytes and Hepatocytes During Exposure to Anthracyclines and Trastuzumab. Int J Nanomedicine. 2020;15:4859–76.
39. Peoples JN, et al. Mitochondrial dysfunction and oxidative stress in heart disease. Exp Mol Med. 2019;51(12):1–13.

Publisher's Note